

SUPPORTING INFORMATION

Materials.

The chemicals were research-grade products with the following stated purity: BF₃ (99.5%), Cyanuric acid (98%). They were purchased from Aldrich and used without further purification. In all experiments, BF₃ was introduced into the ion source through a deactivated silica fused-capillary column. HNCO was prepared in situ by depolymerization of cyanuric acid introduced by a direct insertion probe and heated in vacuo at 280 °C.

Mass Spectrometric Experiments.

Chemical Ionization, CAD (Collisionally Activated Dissociation) and Neutralization-Reionization experiments. The experiments were performed using a modified ZABSpec oa-TOF instrument (VG Micromass) described elsewhere,¹ of EBE-TOF configuration, where E, B stand for electric and magnetic sectors and TOF for orthogonal time-of-flight mass spectrometer. It is fitted with a modified EI-CI (electron ionization-chemical ionization) ion source and five collision cells.

The operating conditions were as follows: accelerating voltage: 8 keV, source temperature: 423 K, repeller voltage: 0 V, emission current: 1 mA, nominal electron energy: 50 eV, source pressure: ca. 0.1-0.15 Torr, as read inside the source block by a Magnehelic differential pressure gauge.

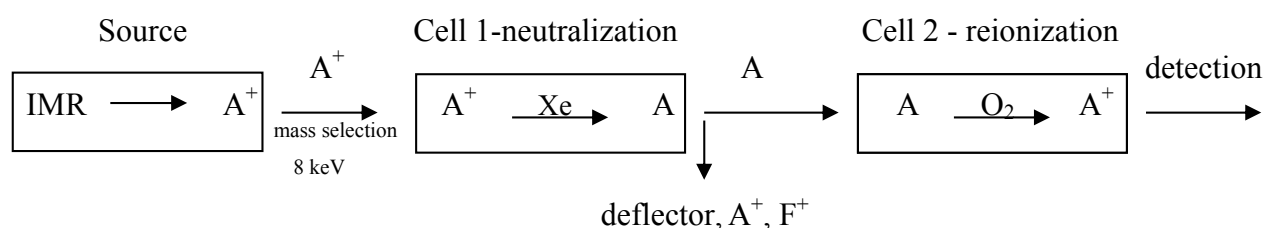
The BF₃/HNCO pressure ratio was estimated to amount to 10/1, which minimizes the effects of the side reactions of BF₃ on the walls without significantly reducing the BF₃ chemical ionization. The chemical ionization (CI) spectrum is shown in Figure 1S. The most representative peaks containing boron are BF₂⁺ (m/z 49, 48), BFNCO⁺ (m/z 72, 71), [BF₂--HNCO]⁺ (m/z 92, 91). The most representative peaks deriving from cyanuric acid ionization are: HNCO⁺ and HNCOH⁺ (m/z 43, 44), (HNCO)₂⁺ (m/z 86), (HNCO)₂H⁺ (m/z 87) and its fragment deriving from the OH loss (m/z 70), (HNCO)₃⁺ and (HNCO)₃H⁺ (m/z 129, 130). Minor peaks are: BF⁺ (m/z 30, 29), BF₃⁺ (m/z 68,

67), $B_2F_5^+$ (m/z 117, 116, 115), $[BF_2-(HNC O)_3]^+$ (m/z 178, 177), the adduct between $(FBNCO)^+$ and cyanuric acid (m/z 201, 200) and its fragment deriving from the HNCO loss (m/z 158, 157).

The peaks of interest at m/z 71 and 72, assigned to the $[^{10}B, F, N, C, O]^+$ and $[^{11}B, F, N, C, O]^+$ ions, respectively, displayed a ratio of 24.4/100 (calculated 24.75/100). The analysis of the elemental composition was accomplished by multistage mass-spectrometry MS^3 . The atomic fragments observed from the dissociation of the peak at m/z 72 were $^{11}B^+$, $^{14}N^+$, $^{12}C^+$ and $^{16}O^+$, those observed from the dissociation of the peak at m/z 71 were $^{10}B^+$, $^{14}N^+$, $^{12}C^+$ and $^{16}O^+$. Due to the presence of the peak at m/z 70 ($H_2, N_2, C_2, O)^+$, the possible contribution of the $(H_2, N_2, C_2, ^{18}O)^+$ and $(H_2, N_2, ^{13}C_2, O)^+$ ions (at the maximum 0,1-0,2 % of m/z 72) was investigated. High-resolution CI spectra were recorded at 20000 FWHM (full width at half maximum), corresponding to 50 ppm, showing no contribution from isobaric peaks which conclusively allows one to exclude isobaric contaminations,

The CAD (collisionally activated dissociation) spectra were recorded at 8 keV in a gas cell located after the magnet in the second field-free region. The CAD/TOF spectra of mass- and energy-selected ions were recorded at 0.8 keV in a gas cell located in the TOF sector. In the CAD experiments, helium was utilized as the target gas in the collision cell; the pressure was chosen to provide 80% transmittance.

The neutralization-reionization (NR) experiments were performed in the pair of cells located after the magnet in the second field-free region of the instrument (8 keV). The cation of interest (denoted as A^+ in the scheme below), generated in the ion source by ion-molecule reaction (IMR), was mass-selected and accelerated to the collision cells.



The experiments involve two subsequent charge-exchange processes corresponding to a reduction-oxidation (NR) sequence. In the first step the mass-selected cation A^+ is reduced to A in the first cell by collision with Xe. At the exit of the cell, all ions are removed by a pair of high-voltage deflecting electrodes, and a beam containing only neutrals enters the second cell. Here A is reionized to A^+ by collision with O_2 (NR). No signal was obtained by switching the deflector on in the absence of the reionizing gas. The vertical, one-electron charge-exchange processes occur in the femtosecond time scale; they are separated by a microsecond time scale which corresponds to the time necessary to travel from the first to the second cell. The neutral molecules are reionized provided that they survive for this time; in such case, a "recovery" peak at the same m/z ratio as the original ion is detected. The time window corresponding to the time required to go from the neutralization to the reionization cell gives the minimum lifetime of the neutral species detected, that is, the time it lives before being reionized.

Gas pressures were set to achieve a beam transmittance of 80-90%, under near-single collision conditions. All NR spectra were averaged over 100 acquisitions to improve the signal-to-noise ratio. The recovery peak of the NR spectra was further analyzed in the TOF sector, and the CAD/TOF spectrum proved to be the same as that of the precursor ions.

TQMS (triple quadrupole mass spectrometry) experiments. The energy resolved mass spectra were obtained by using a TSQ700 mass spectrometer from Finnigan Ltd. The energy-resolved CAD spectra were recorded using Ar as the target gas at pressures of about 0.1 mTorr and at collision energies ranging from 0 to 50 eV (laboratory frame). An upper limit of 2 eV for the kinetic energy of the reactant ion at nominal collision energy of 0 eV (laboratory frame) and an ion-beam energy spread of about 1 eV can be estimated by using cut-off potentials. Laboratory ion energies (lab) are converted to center-of-mass (CM) energies by using the formula $E_{CM} = E_{LAB} m/(m + M)$, where m is the mass of neutral reactant and M is the mass of the ionic reagent. Experimental cross sections, σ_{tot} , were determined by the relation $I_R/I_{tot} = \exp(-\sigma n l)$ where I_R is the intensity of the transmitted ion beam, I_{tot} is the total ion intensities, n is the number density of the neutral gas and l is the effective

gas cell length. Individual product cross sections (σ_p) were calculated by $\sigma_p = \sigma_{\text{tot}}(I_p/I_{\text{ptot}})$ where I_p represents the intensity of the product ion and I_{ptot} the total product ion intensities.

Computational analysis.

The potential energy surfaces of $[\text{F}_2\text{B--HNCO}]^+$, $[\text{F,B,N,C,O}]^+$ and $[\text{F,B,N,C,O}]$ were investigated by locating the lowest stationary points at the B3LYP² level of theory in conjunction with the correlation consistent valence polarized set aug-cc-pVTZ.³ At the same level of theory we computed the harmonic vibrational frequencies in order to check the nature of the stationary points, *i.e.* minimum if all the frequencies are real, saddle point if there is one, and only one, imaginary frequency. The frequencies relevant to all the stationary points are reported in Table S1 and S2, and the Cartesian coordinates are reported in tables S3 and S4. The assignment of the saddle points was performed using intrinsic reaction coordinate (IRC) calculations.⁴ The energy of all the stationary points was computed at the higher level of calculation CCSD(T)⁵ using the same basis set aug-cc-pVTZ. Both the B3LYP and the CCSD(T) energies were corrected to 298.15 K by adding the zero point energy and the thermal corrections computed using the scaled harmonic vibrational frequencies evaluated at B3LYP/aug-cc-pVTZ level. All calculations were performed using Gaussian 09⁶ while the analysis of the vibrational frequencies was performed using Molekel.⁷

The theoretical analysis preliminarily considered the interaction between BF_2^+ and HNCO, that gives rise to the minimum **A** with a B—N bond and an interaction energy of 76.3 kcal mol⁻¹ with respect to the reactants (Figure 2S). This minimum, as well as all the other minima considered in this work, is obtained performing a full geometry optimization without any symmetry constraints, followed by a frequency calculation to check if it is a true minimum (all real frequencies). The minimum **A** isomerizes to a second minimum **B** where the hydrogen, originally bonded to nitrogen, is coordinated to a fluorine atom. The transition state connecting these two minima has been found using the Gaussian QST2 and QST3 options, as done for all the other transition states, followed by a frequency calculation to check the nature of the stationary point (all real frequencies, except one,

which is imaginary). The minimum **B** dissociates into HF and an ion of connectivity F-B-N-C-O, that is the ion **1**⁺ corresponding to the initially formed ion. The minima and the saddle point are all located below the reactants, and the overall process to **1**⁺ is exothermic by 19.7 kcal mol⁻¹.

On the ionic potential energy surface, as possible isomers of this open-chain species, we have investigated structures having FBNCO, FBOCN, FBNOC and FBONC connectivity, branched-chain structures FBN(C)O, FBO(C)N, FB(N)CO, FB(O)CN, three, four- and five-atom cyclic structures. No branched-chain and cyclic structures have been found. Three open-chain ions have been located at higher energy with respect to FBNCO⁺ (**1**⁺): FBOCN⁺ (58.7 kcal mol⁻¹) (**2**⁺), FBONC⁺ (117.9 kcal mol⁻¹) (**2b**⁺), FBNOC⁺ (130.4 kcal mol⁻¹) (**1b**⁺) (Figure 3S). No saddle point has been identified connecting **1**⁺ and **2**⁺, whereas saddle points for the isomerization **1**⁺ → **1b**⁺ and for the isomerization **2**⁺ → **2b**⁺ have been located 136.1 and 123.9 kcal mol⁻¹ above **1**⁺, respectively.

On the neutral potential energy surface, four isomers having the FBNCO (**1** and **1a**) and FBOCN (**2** and **2a**) connectivity, the four-atom cyclic structure **3** and the branched-chain FB(O)CN (**4**) have been found (Figure 3S). All isomers are higher in energy than **1**, but **4** which is located 0.9 kcal mol⁻¹ below **1**. The geometry of the saddle points located on the ionic and neutral surfaces are reported in Figure 4S.

- 1 F. Bernardi, F. Cacace, G. de Petris, F. Pepi, I. Rossi, A. Troiani, *Chem. Eur. J.*, 2000, **6**, 537
- 2 A. D. Becke, *J. Chem. Phys.*, 1993, **98**, 5648; P. J. Stephens, F. J. Devlin, C. F. Chabalowski, and M. J. Frisch, *J. Phys. Chem.*, 1994, **98**, 11623.
- 3 T. H. Dunning Jr. *J. Chem. Phys.*, 1989, **90**, 1007; D. E. Woon and T. H. Dunning Jr. *J. Chem. Phys.*, 1993, **98**, 1358; R. A. Kendall, T. H. Dunning Jr., and R. J. Harrison, *J. Chem. Phys.*, 1992, **96**, 6796.
- 4 C. Gonzales and H. B. Schlegel, *J. Chem. Phys.*, 1989, **90**, 1989, 2154; C. Gonzales and H. B. Schlegel, *J. Phys. Chem.*, 1990, **94**, 5523.

- 5 R. J. Bartlett, *Annu. Rev. Phys. Chem.*, 1981, **32**, 359; K. Raghavachari, G. W. Trucks, J. A. Pople, and M. Head-Gordon, *Chem. Phys Lett.*, 1989, **157**, 479; J. Olsen, P. Jorgensen, H. Koch, A. Balkova, and R. J. Bartlett, *J. Chem. Phys.*, 1996, **104**, 8007.
- 6 Gaussian 09, Revision A.02, M. J. Frisch, G. W. Trucks, H. B. Schlegel, G. E. Scuseria, M. A. Robb, J. R. Cheeseman, G. Scalmani, V. Barone, B. Mennucci, G. A. Petersson, H. Nakatsuji, M. Caricato, X. Li, H. P. Hratchian, A. F. Izmaylov, J. Bloino, G. Zheng, J. L. Sonnenberg, M. Hada, M. Ehara, K. Toyota, R. Fukuda, J. Hasegawa, M. Ishida, T. Nakajima, Y. Honda, O. Kitao, H. Nakai, T. Vreven, J. A. Montgomery, Jr., J. E. Peralta, F. Ogliaro, M. Bearpark, J. J. Heyd, E. Brothers, K. N. Kudin, V. N. Staroverov, R. Kobayashi, J. Normand, K. Raghavachari, A. Rendell, J. C. Burant, S. S. Iyengar, J. Tomasi, M. Cossi, N. Rega, J. M. Millam, M. Klene, J. E. Knox, J. B. Cross, V. Bakken, C. Adamo, J. Jaramillo, R. Gomperts, R. E. Stratmann, O. Yazyev, A. J. Austin, R. Cammi, C. Pomelli, J. W. Ochterski, R. L. Martin, K. Morokuma, V. G. Zakrzewski, G. A. Voth, P. Salvador, J. J. Dannenberg, S. Dapprich, A. D. Daniels, O. Farkas, J. B. Foresman, J. V. Ortiz, J. Cioslowski, and D. J. Fox, Gaussian, Inc., Wallingford CT (2009).
- 7 MOLEKEL 4.3, P. Flükiger, H. P. Lüthi, S. Portmann, and J. Weber, Swiss Center for Scientific Computing, Manno (Switzerland), 2000-2002. S. Portmann and H. P. Lüthi, *Chimia*, **54**, 766 (2000).

FIGURE CAPTIONS

Fig. 1S: Chemical ionization (CI) mass spectrum of BF_3/HNCO . See text for the assignment of the peaks. Peaks denoted by * from the bleeding due to BF_3 .

Fig. 2S: Geometries of the minima and the saddle point identified by interaction of BF_2^+ and HNCO at the B3LYP/aug-cc-pVTZ level of theory. Bond lengths in Å and angles in degrees. ΔH values (kcal mol^{-1}) computed at CCSD(T)/aug-cc-pVTZ level of theory.

Fig. 3S: Geometries of the minima located on the $[\text{B}, \text{C}, \text{N}, \text{O}, \text{F}]^+$ and $[\text{B}, \text{C}, \text{N}, \text{O}, \text{F}]$ potential energy surfaces optimized at the B3LYP/aug-cc-pVTZ level of theory. Bond lengths in Å and angles in degrees. ΔH values (kcal mol^{-1}) computed at CCSD(T)/aug-cc-pVTZ level of theory, relative to the ion $\mathbf{1}^+$ and the neutral $\mathbf{1}$.

Fig. 4S: Geometries of the saddle points located on the $[\text{B}, \text{C}, \text{N}, \text{O}, \text{F}]^+$ and $[\text{B}, \text{C}, \text{N}, \text{O}, \text{F}]$ potential energy surfaces optimized at the B3LYP/aug-cc-pVTZ level of theory. Bond lengths in Å and angles in degrees. ΔH values (kcal mol^{-1}) computed at CCSD(T)/aug-cc-pVTZ level of theory, relative to the ion $\mathbf{1}^+$ and the neutral $\mathbf{1}$.

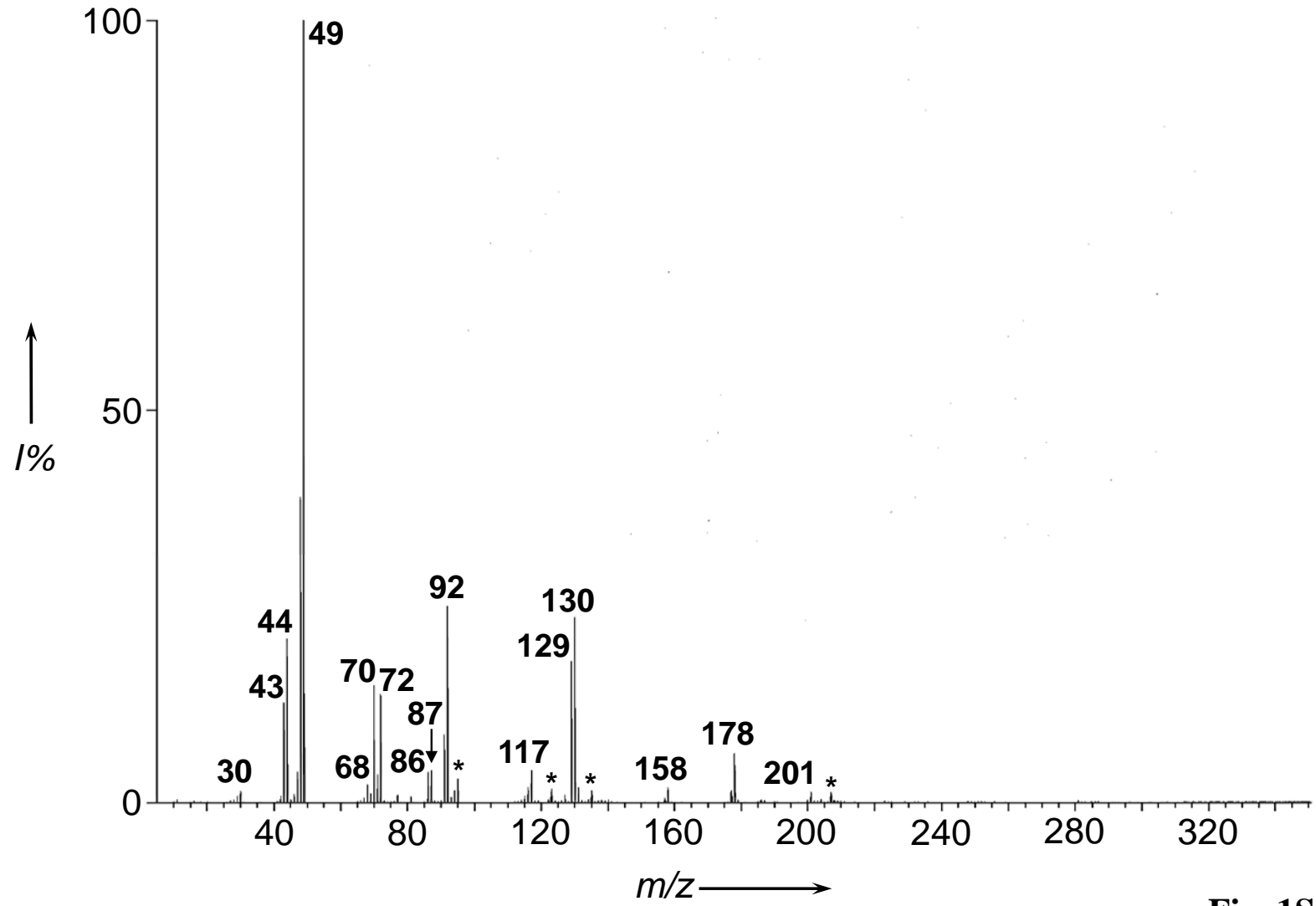


Fig. 1S

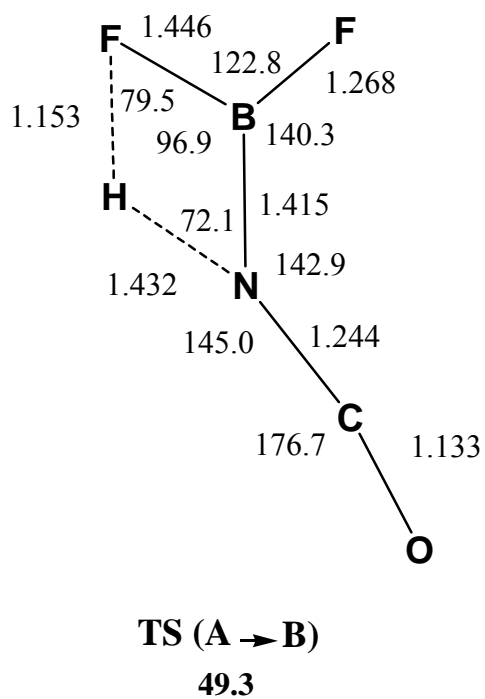
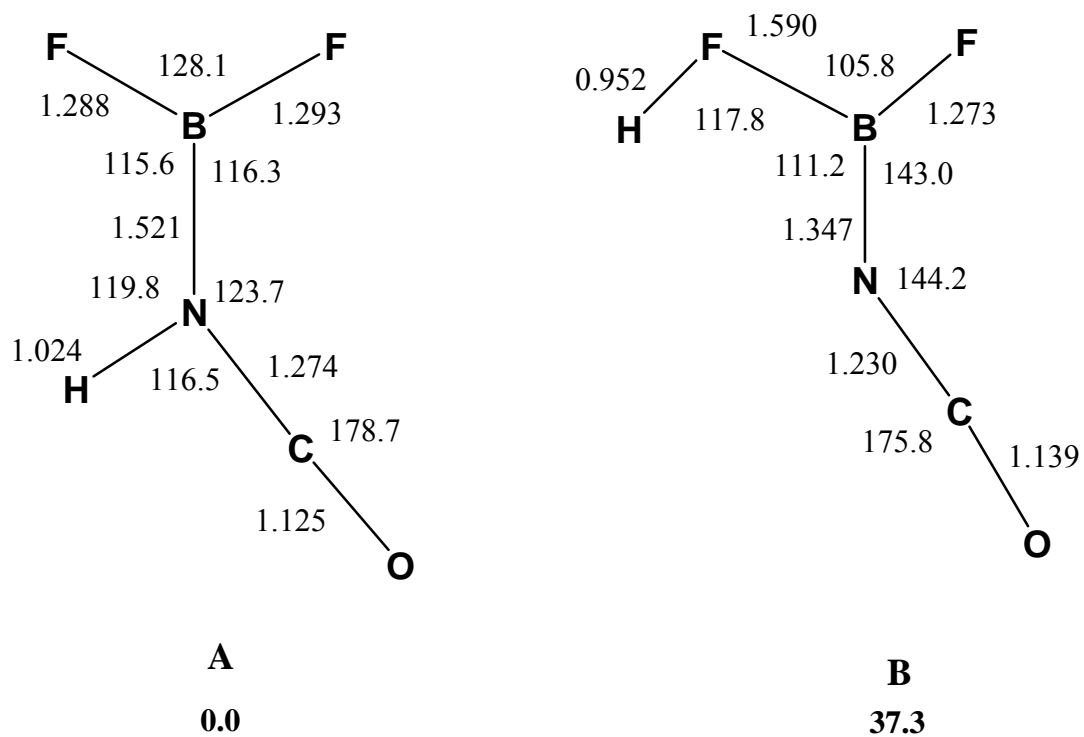
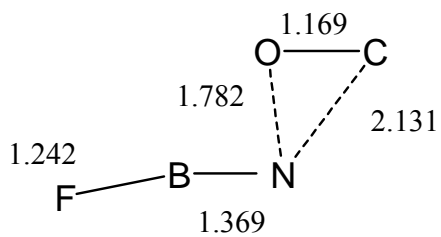
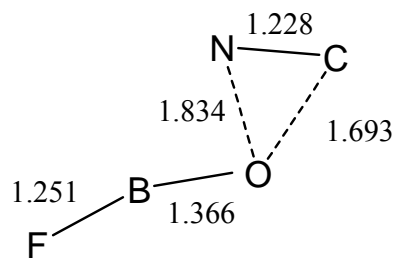


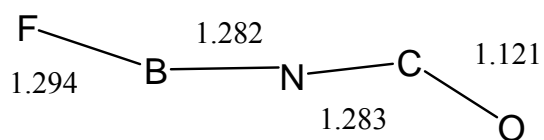
Fig. 2S



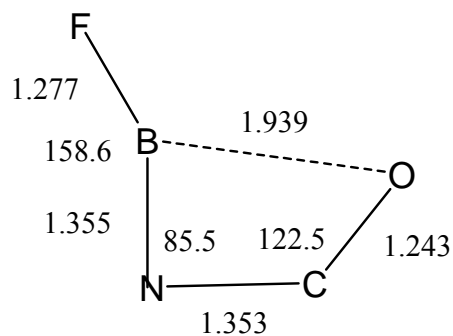
TS $1^+ \rightarrow 1b^+$
136.1



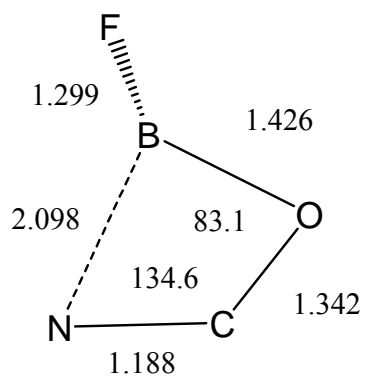
TS $2^+ \rightarrow 2b^+$
123.9



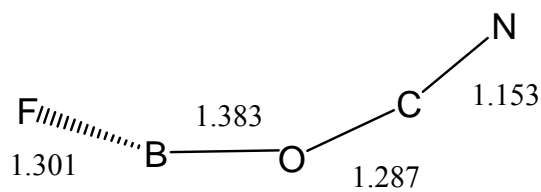
TS $1 \rightarrow 1a$
(21.0)



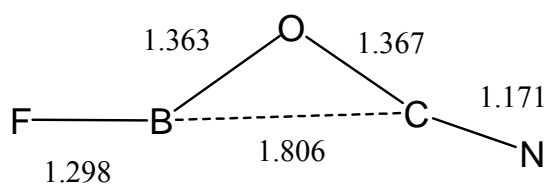
TS $1a \rightarrow 3$
(36.4)



TS $3 \rightarrow 2$
(53.1)



TS $2 \rightarrow 2a$
(29.8)



TS $2 \rightarrow 4$
(38.7)

Fig. 4S

Table S1: Total energies and vibrational frequencies (intensities) of the stationary points optimized on the PES of FBNCO^+ and FBNCO . Energies in hartree, frequencies in cm^{-1} , intensities in km/mol .

	I^+ ${}^1\Sigma^+$	2^+ ${}^1\Sigma^+$	Ib^+ ${}^1A'$	$2b^+$ ${}^1A'$	$TS(I^+ \rightarrow Ib^+)$ 1A	$TS(2^+ \rightarrow 2b^+)$ 1A
E_{B3LYP}	-292.645069	-292.543700	-292.428186	-292.447025	-292.410310	-292.425429
ZPE^a	0.020449	0.018589	0.016160	0.016477	0.014085	0.014642
$E_{CCSD(T)}$	-292.126590	-292.031902	-291.914857	-291.935282	-291.903677	-291.922864
π	85.8 (0.4)	π 28.4 (1.9)	a' 130.9 (6.2)	a' 96.9 (4.7)	a 261.1i	a 526.3i
			a'' 233.1 (1.8)	a'' 116.4 (9.5)	a 28.7 (1.6)	a 151.8 (1.7)
π	434.0 (86.0)	π 380.7 (69.0)	a' 284.5 (5.2)	a' 214.2 (7.7)	a 107.6 (7.1)	a 352.5 (14.0)
			a'' 417.3 (63.1)	a'' 410.4 (96.6)	a 414.2 (38.4)	a 481.8 (69.5)
π	595.9 (30.9)	π 402.8 (32.8)	a' 516.6 (56.6)	a' 470.9 (84.0)	a 416.0 (54.2)	a 561.1 (89.9)
			a' 579.2 (1.6)	a' 697.2 (34.1)	a 494.0 (71.8)	a 596.7 (17.0)
σ	728.9 (0.5)	σ 692.7 (3.4)	a' 1105.8 (4.5)	a' 1152.4 (68.3)	a 989.0 (1.1)	a 919.8 (14.9)
σ	1473.2 (12.4)	σ 1303.5 (1.7)	a' 1885.5 (929.4)	a' 1989.7 (1050.1)	a 1837.8 (717.3)	a 1621.0 (10.1)
σ	2090.7 (963.1)	σ 2128.4 (1024.0)	a' 1940.7 (9.3)	a' 2084.5 (15.2)	a 1895.3 (1.7)	a 1742.4 (566.4)
σ	2451.8 (1425.2)	σ 2411.3 (64.9)				

	1 ${}^2A'$		$1a$ ${}^2A'$		2 ${}^2A'$		$2a$ ${}^2A'$		3 ${}^2A'$		4 ${}^2A'$	
E_{B3LYP}	-292.918257		-292.891749		-292.871738		-292.869232		-292.868376		-292.909269	
ZPE^a	0.018334		0.017428		0.017750		0.022590		0.017363		0.017245	
$E_{CCSD(T)}$	-292.396739		-292.368502		-292.359202		-292.356774		-292.358497		-292.396949	
a''	96.9 (0.3)	a''	106.1 (0.002)	a''	133.9 (6.8)	a'	132.4 (2.5)	a''	205.7 (1.5)	a'	163.0 (9.1)	
a'	119.5 (1.3)	a'	125.1 (0.5)	a'	164.0 (6.6)	a''	229.3 (0.0)	a'	399.2 (0.8)	a''	247.6 (18.5)	
a'	430.0 (9.5)	a'	370.1 (32.7)	a'	445.5 (6.7)	a'	433.7 (9.7)	a'	554.1 (26.9)	a'	343.7 (5.9)	
a'	606.9 (18.4)	a''	457.6 (51.2)	a''	512.7 (4.6)	a''	515.1 (10.3)	a''	646.4 (56.7)	a'	484.3 (1.5)	
a''	637.8 (22.8)	a'	541.2 (1.7)	a'	538.1 (3.2)	a'	659.9 (15.5)	a'	649.3 (5.5)	a''	635.3 (40.7)	
a'	910.1 (74.9)	a'	807.5 (40.6)	a'	980.0 (67.6)	a'	932.5 (19.7)	a'	908.7 (31.4)	a'	716.8 (20.2)	
a'	1309.9 (360.6)	a'	1275.8 (14.4)	a'	1242.7 (121.0)	a'	1191.3 (211.0)	a'	1068.2 (189.6)	a'	1211.5 (153.6)	
a'	1572.5 (221.1)	a'	1870.3 (407.7)	a'	1388.6 (611.8)	a'	1382.8 (435.4)	a'	1519.0 (472.6)	a'	1435.5 (255.4)	
a'	2364.2 (1446.1)	a'	2096.3 (926.7)	a'	2385.8 (177.0)	a'	2368.3 (114.2)	a'	1671.1 (101.3)	a'	2332.2 (81.7)	

	$TS(1 \rightarrow 1a)$ 2A		$TS(1a \rightarrow 3)$ 2A		$TS(3 \rightarrow 2)$ 2A		$TS(2 \rightarrow 2a)$ 2A		$TS(2 \rightarrow 4)$ 2A
E_{B3LYP}	-292.888679		-292.850167		-292.820902		-292.861410		-292.846898
ZPE^a	0.016023		0.016233		0.015894		0.017131		0.015808
$E_{CCSD(T)}$	-292.360930		-292.335875		-292.309327		-292.347417		-292.332055
a	552.9i	a	406.5i	a	578.2i	a	193.2i	a	583.1i
a	82.5 (0.4)	a	182.0 (1.5)	a	180.9 (8.6)	a	144.3 (2.1)	a	176.6 (12.9)
a	128.2 (0.6)	a	295.5 (7.9)	a	396.7 (9.2)	a	447.6 (15.0)	a	283.6 (13.0)
a	457.2 (46.5)	a	561.0 (52.8)	a	476.5 (32.6)	a	466.9 (8.1)	a	458.9 (0.1)
a	479.6 (11.0)	a	686.2 (0.01)	a	664.1 (46.9)	a	539.6 (8.0)	a	483.6 (27.4)
a	810.4 (15.5)	a	990.8 (5.8)	a	779.5 (5.7)	a	911.6 (60.1)	a	894.4 (40.7)
a	1208.3 (276.8)	a	1169.4 (206.4)	a	1107.2 (77.6)	a	1247.8 (125.0)	a	1085.8 (99.3)
a	1860.3 (98.2)	a	1515.9 (273.5)	a	1382.7 (401.2)	a	1381.7 (644.0)	a	1471.4 (395.8)
a	2006.5 (741.9)	a	1724.6 (431.1)	a	1989.4 (119.5)	a	2380.3 (242.4)	a	2084.6 (43.6)

^a Zero point energy.

Table S2: Total energies and vibrational frequencies (intensities) of the A and B minima and the transition state interconnecting them. Energies in hartree, frequencies in cm^{-1} , intensities in km/mol .

	A ${}^1A'$		B ${}^1A'$		TS(A→B) ${}^1A'$
E_{B3LYP}	-393.218574		-393.163031		-393.140185
ZPE^a	0.035294		0.033156		0.030122
$E_{CCSD(T)}$	-392.569431		-392.508356		-392.485367
a''	104.2 (10.6)	a'	94.3 (4.8)	a	1425.4 <i>i</i>
a'	125.6 (4.7)	a''	116.0 (0.1)	a''	120.4 (0.7)
a'	361.4 (3.1)	a'	292.2 (7.6)	a'	130.2 (3.4)
a'	433.3 (27.8)	a''	335.3 (159.7)	a'	394.2 (13.3)
a''	503.3 (26.3)	a'	413.8 (1.0)	a''	507.6 (15.7)
a''	594.4 (0.1)	a'	524.1 (162.2)	a'	556.3 (2.7)
a'	633.1 (31.8)	a''	553.3 (77.0)	a''	615.9 (35.5)
a''	654.0 (169.9)	a''	627.5 (42.9)	a'	648.1 (3.1)
a'	823.4 (17.1)	a'	647.1 (116.1)	a'	759.6 (52.1)
a'	1211.2 (59.7)	a'	769.8 (136.9)	a''	935.3 (154.9)
a'	1224.3 (311.4)	a'	898.1 (285.3)	a'	1068.6 (774.7)
a'	1383.4 (270.2)	a'	1416.9 (99.3)	a'	1442.3 (152.2)
a'	21615.3 (404.3)	a'	1796.6 (833.2)	a'	1663.6 (961.7)
a'	2393.1 (499.4)	a'	2403.1 (1179.3)	a'	1984.3 (67.4)
a'	3432.3 (266.0)	a'	3665.8 (385.3)	a'	2395.8 (846.9)

^a Zero point energy.

Table S3. Optimized Cartesian coordinates (Å) of the stationary points optimized on the PES of FBNCO⁺ and FBNCO.

	X	Y	Z
1⁺			
F	0.000000	0.000000	2.447730
B	0.000000	0.000000	1.203644
N	0.000000	0.000000	-0.084380
C	0.000000	0.000000	-1.313923
O	0.000000	0.000000	-2.446700
2⁺			
F	0.000000	0.000000	2.377043
B	0.000000	0.000000	1.137364
O	0.000000	0.000000	-0.100208
C	0.000000	0.000000	-1.402726
N	0.000000	0.000000	-2.551740
1b⁺			
F	-2.171008	-0.664186	0.000000
B	-1.050088	-0.120690	0.000000
N	0.000000	0.702321	0.000000
O	1.273394	0.141690	0.000000
C	2.433726	0.088559	0.000000
2b⁺			
F	-2.106326	-0.854092	0.000000
B	-1.025507	-0.253787	0.000000
O	0.000000	0.487808	0.000000
N	1.323626	0.235545	0.000000
C	2.469847	0.567415	0.000000

TS(1⁺→1b⁺)			
F	2.085993	-0.283839	0.001707
B	0.949827	0.218693	0.000930
N	-0.225792	0.919737	-0.003040
C	-2.141295	-0.014218	0.006610
O	-1.136844	-0.611472	-0.004800

TS(2⁺→2b⁺)			
F	-1.772271	-0.157048	0.096336
B	-0.547042	0.055655	-0.037429
O	0.453558	0.981693	-0.116701
C	1.626617	-0.159116	0.319152
N	0.756783	-0.823385	-0.237311

1			
F	2.271947	-0.576772	0.000000
B	0.988552	-0.848965	0.000000
N	0.000000	0.149352	0.000000
C	-1.176549	0.412994	0.000000
O	-2.291373	0.739043	0.000000

1a			
F	-0.476934	-2.406725	0.000000
B	-0.234764	-1.144061	0.000000
N	0.000000	0.090167	0.000000
C	0.615455	1.271226	0.000000
O	0.221687	2.390288	0.000000

2			
F	-2.205708	-0.231502	0.000000
B	-0.954285	-0.585764	0.000000
O	0.000000	0.412623	0.000000
C	1.277710	0.198667	0.000000
N	2.422362	0.074193	0.000000

2a				
F	-1.580038	-0.827244	0.000000	
B	-1.291554	0.444245	0.000000	
O	0.000000	0.916531	0.000000	
C	1.064389	0.165973	0.000000	
N	2.041683	-0.443445	0.000000	

3				
F	-0.027185	1.665895	0.000000	
B	0.000000	0.368066	0.000000	
O	-1.066669	-0.543199	0.000000	
C	0.129755	-1.353399	0.000000	
N	1.142784	-0.624030	0.000000	

4				
F	-1.116834	1.190269	0.000000	
B	0.000000	0.490662	0.000000	
O	1.209838	1.075646	0.000000	
N	0.039634	-2.206100	0.000000	
C	0.015895	-1.054700	0.000000	
O	2.426606	-0.112454	-0.002833	

TS(1→1a)				
F	-2.442588	0.069572	-0.002275	
B	-1.185024	-0.234954	0.000648	
N	0.083328	-0.047470	0.005065	
C	1.318713	0.296757	0.000741	
O	2.426606	-0.112454	-0.002833	

TS(1a→3)

F	-1.719286	-0.223859	0.000418
B	-0.535342	0.255541	-0.000874
N	0.449132	1.186501	-0.000323
C	1.298520	0.132752	0.001080
O	0.901906	-1.045625	-0.000452

TS(3→2)

F	-1.647427	-0.356368	-0.149985
B	-0.555152	0.030692	0.437795
O	0.251386	1.126230	0.010889
C	1.152902	0.160662	-0.226524
N	1.239157	-0.988566	0.061847

TS(2→2a)

F	1.987725	-0.470667	-0.089815
B	1.150575	0.392048	0.408388
O	-0.074435	0.630695	-0.187262
C	-1.213019	0.048203	-0.041415
N	-2.252686	-0.437002	0.073283

TS(2→4)

F	2.026400	-0.305584	-0.002525
B	0.731067	-0.230127	0.006874
O	-0.047654	0.888028	-0.000588
C	-1.063807	-0.025880	0.000864
N	-2.161265	-0.435436	-0.001732

Table S4. Optimized Cartesian coordinates (Å) of the **A** and **B** minima and the transition state interconnecting them.

	X	Y	Z
A			
F	-2.155714	-0.187335	0.000000
B	-0.888291	-0.414941	0.000000
F	-0.283212	-1.557841	0.000000
N	0.000000	0.819371	0.000000
C	1.273416	0.773068	0.000000
O	2.396878	0.707018	0.000000
H	-0.423731	1.751149	0.000000
B			
F	1.903582	-0.935475	0.000000
B	0.325553	-0.737055	0.000000
F	-0.171041	-1.909354	0.000000
N	0.000000	0.569874	0.000000
C	-0.939865	1.363183	0.000000
O	-1.753780	2.159424	0.000000
H	2.448805	-0.154879	0.000000
TS (A→B)			
F	-1.915832	-0.434276	0.000000
B	-0.515255	-0.795211	0.000000
F	-0.115919	-1.998270	0.000000
N	0.000000	0.522971	0.000000
C	1.060596	1.173216	0.000000
O	1.990993	1.819699	0.000000
H	-1.429490	0.611291	0.000000

